Properties of the solid solution $(Cd_{0.69}Zn0._{31})_3As_2$

V.S. Zakhvalinskii*[1], A.V. Borisenko[1], T.B. Nikulicheva [1], A. V. Kochura[2], Aung Zaw Htet [2], E.A.Pilyuk[1]

[1]Belgorod State National Research University, 85, Pobedy St., 308015 Belgorod, Russia

[2] South-West State University, Regional Centre of Nanotechnology, 94 50 Let Octjabrja Str., Kursk 305040, Russia

*e-mail: v_zaxval@mail.ru

Abstract

Recent studies of Cd_3As_2 have revealed the topological aspect of its electrical properties. At the same time, the attention of researchers is attracted by the study of the properties of solid solutions of the Dirac semimetal Cd_3As_2. The modified Bridgeman method was used to obtain single crystals of $(Cd_{0.69}Zn_{0.31})_3As_2$. It has been established that the studied sample crystallizes in space group $P4_2/nmc$ with lattice parameters a = 8.78 Å, b = 12.42 Å. We have investigated the electrical conductivity in the temperature range from 10 to 300 K and in a magnetic field of 1 T, and determined the temperature dependences of the concentration and mobility of charge carriers. It has been established that in the temperature range from 10 to 33 K, hopping conduction with a variable length of the Mott-type hoping takes place, and its micro parameters have been determined.

Keywords: Dirac semimetal Cd_3As_2, solid solutions, hopping conductivity, single crystals

1.Introduction

Among topological materials, the narrow-gap semiconductor cadmium arsenide (Cd_3As_2) with an inverted structure of energy bands and the highest carrier mobility among semiconductors and semimetals (largely exceeding 10^4 $cm^2/(V·s)$ at the room temperature) is distinguished by its chemical stability, low toxicity, and good manufacturability [1,2]. Cd_3As_2 was believed to manifest an inverted band structure due to the spin-orbital coupling (SOC) [3]. The 3D Dirac cones of Cd_3As_2 have been observed in angle-resolved photoemission spectroscopy (ARPES) [2,4,5]. At low Zn content vapor phase synthesized $(Cd_{1-x}Zn_x)_3As_2$ (CZA) single crystals are demonstrated the Dirac semimetal phase [6 - 8]. Within $0.3 \leq x \leq 0.5$ composition region a transition from an inverted band structure is expected, accompanied by a transition from a topological phase to a trivial band semiconductor [7, 8].

2. Experiment

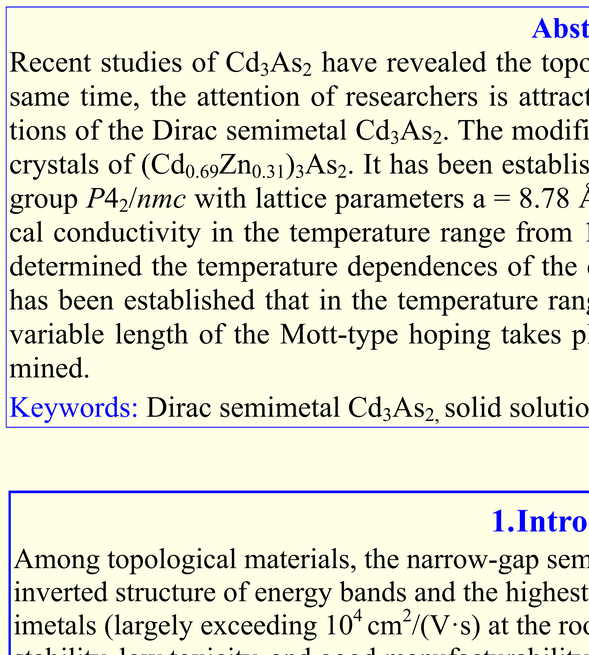

Fig. 1. The spectrum of EDX from the surface of $(Cd_{1-x}Zn_x)_3As_2$ corresponds to the composition (x=0.31)

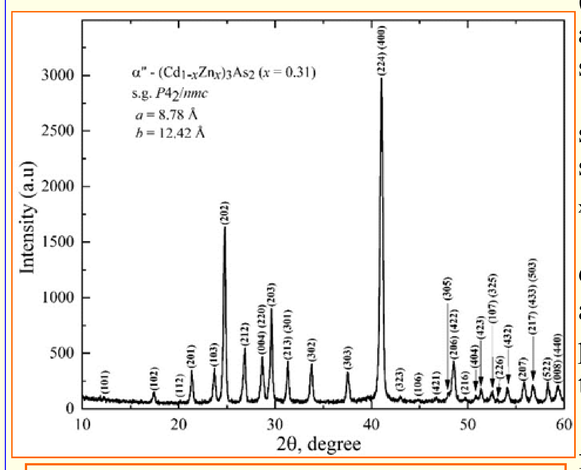

Fig.2. Powder diffraction pattern of the $(Cd_{1-x}Zn_x)_3As_2$ sample.

The modified Bridgman method was used to obtain CZA single crystals. Stoichiometric amounts of Cd_3As_2 and Zn_3As_2 binary compounds were placed in a graphitized and evacuated quartz ampoule. The CZA melt was slowly cooled from the melting temperature of 838°C at a rate of 5°C/h in the furnace temperature gradient.

The composition of the samples and their homogeneity were controlled by powder x-ray diffraction and energy dispersive x-ray spectroscopy (EDX). X-ray phase analysis (XPA) of the sample was performed using a GBC EMMA X-ray diffractometer (Cu Ka radiation, λ = 1.5401 Å) at the room temperature. It has been established that the studied sample crystallizes in space group $P4_2/nmc$ with lattice parameters a = 8.78 Å, b = 12.42 Å [9]. To study the composition and distribution of elements on the surface, we used a JSM-6610LV (Jeol) scanning electron microscope (SEM) with an X-Max^N (Oxford Instruments) energy dispersive X-ray spectroscopy (EDX) attachment.

Figure 1 shows the EDX spectrum from the surface of the $(Cd_{1-x}Zn_x)_3As_2$ sample. Figure 2 shows the powder diffraction pattern of the $(Cd_{1-x}Zn_x)_3As_2$ sample.

Samples for the study of electrical conductivity by the six-probe method were parallelepipeds 1.35×0.67×0.50mm. The temperature dependence of electrical conductivity was studied in the temperature range from 10 to 300K, and the Hall effect in a magnetic field 1T.

The results of the study of the temperature dependence of the resistivity of a solid solution single crystal $(Cd_{0.69}Zn_{0.31})_3As_2$ are shown in Figure 3. In the inset to Figure 3, the section corresponding to the variable range of the hopping conductivity according to Mott is highlighted.

3. Results and discussions

As the temperature decreases from 320 K, the resistivity decreases from $2·10^{-3}$ Ω·cm at 300 K to a minimum of $5·10^{-4}$ Ω·cm at 30 K, and then gradually increases. This behavior is typical of the Anderson transition [10]. The study of the Hall Effect in a magnetic field of 1 T made it possible to calculate the Hall coefficient RH, the concentration and mobility of charge carriers. At a temperature of 10 K, the concentration of charge carriers was equal to $2.81·10^{17}$ cm^{-3}, decreasing with increasing temperature to 30 K corresponding to the metal-insulator transition. Above 30 K, an activation increase in the concentration of charge carriers was observed, which is typical for impurity semiconductors up to a value of $3.05·10^{17}$ cm^{-3}. The mobility of charge carriers, m, exhibits behavior characteristic of semiconductors, increasing with decreasing temperature. The value of mobility is maximum at the metal-dielectric transition point at a temperature of 30 K and is $4.51·104$ cm^2 V^{-1} s^{-1}. A further decrease in temperature leads to a decrease in mobility to $4.16·10^4$ cm^2 V^{-1} s^{-1} at a temperature of 10 K. The mechanisms of charge carrier scattering were evaluated.

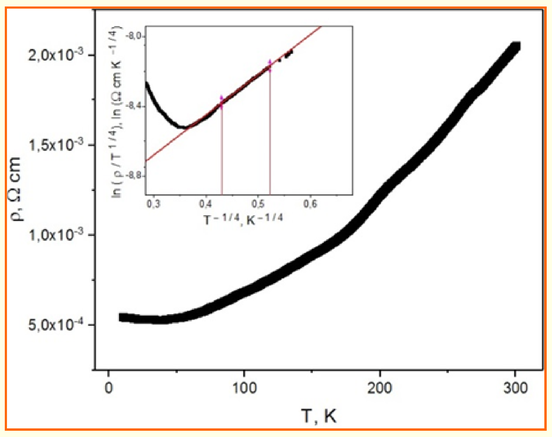

Fig. 3. Temperature dependence of the resistivity of $(Cd_{0.69}Zn_{0.31})_3As_2$ solid solution single crystal. The temperature range 10-33 K on the Fig. 3. insert corresponding to Mott variable range. hopping conductivity.

At low temperatures, in the temperature range from 10 to 30 K, scattering by ionized impurity atoms and mobility $m \sim T^{3/2}$ prevail. In the temperature range from 30 to 300 K, scattering by thermal vibrations of the crystal lattice, $\mu \sim T^{-3/2}$, predominates. In the inset to Fig.3 a linear section of the temperature dependence of the resistivity in the temperature range from 10 to 33 K, corresponding to the mechanism of hopping conduction by the states of the impurity band, is distinguished. Hopping conductivity is described by the universal equation [10-12]:

$$\rho(T) = DT^m \exp\left(\frac{T_0}{T}\right)^p$$

where D is a constant coefficient, T_0 is the characteristic temperature, and the parameters m and p depend on the mechanism of hopping conduction. We have determined the values of the parameters m=1/4 and p = 1/4, which indicates the predominance of the mechanism of hopping conduction with a variable range hop according to Mott. Calculating the microparameters, the following obtained values of the coefficients were used: the characteristic temperature of the hopping conductivity T_0 = 28.60 K; hopping conduction onset temperature T_V = 28.44; coefficient $D = 8.488·10^{-5}$. For hopping conduction with a variable hop length, the following values of microparameters were obtained: Coulomb gap width in the density of localized states Δ = 0.43 meV; acceptor zone width W = 2.45 meV; the value of the density of localized states outside the parabolic gap $g = 2.93·10^{17}$ cm^{-3} meV^{-1}; charge carrier localization radius a = 307 Å.

4. Conclusions

Single crystals of $(Cd_{0.69}Zn_{0.31})_3As_2$ solid solutions were obtained by the modified Bridgman method. The sample composition and the element distribution was controlled using JSM -6610LV (Jeol) scanning electron microscope (SEM) with an X-MaxN (Oxford Instruments) energy dispersive X-ray spectroscopy (EDX) attachment.

It has been established that the studied sample crystallizes in space group $P4_2/nmc$ with lattice parameters a = 8.78 Å, b = 12.42 Å. We have investigated the electrical conductivity in the temperature range from 10 to 300 K and in a magnetic field of 1 T, and determined the temperature dependences of the concentration and mobility of charge carriers. It has been established that in the temperature range from 10 to 33 K, hopping conduction with a variable range of the Mott-type hop takes place, and its micro parameters have been determined.

References

[1]. Jeon, S.; Zhou, B. B.; Gyenis, A.; Feldman, B. E.; Kimchi, I.;Potter, A. C.; Gibson, Q. D.; Cava, R. J.; Vishwanath, A.; Yazdani, A.Nature Materials. 13(2014)851.
[2]. Neupane, M.; Xu, S.-Y.; Sankar, R.; Alidoust, N.; Bian, G.; Liu, C.; Belopolski, I.; Chang, T.-R.; Jeng, H.-T.; Lin, H.; Bansil, A.; Chou, F.; Hasan, M. Z. Nature Commun. 5(2014)3786.
[3]. Aubin, M. J., Caron, L. G. & Jay-Gerin, J. P Phys. Rev. B 15(1977)3872.
[4]. Z. K. Liu, J. Jiang, B. Zhou, Z. J. Wang, Y. Zhang, H. M. Weng, D. Prabhakaran, S-K. Mo, H. Peng, P. Dudin, T. Kim, M. Hoesch, Z. Fang, X. Dai, Z. X. Shen, D. L. Feng, Z. Hussain & Y. L. Chen. Nat. Mater. 13(2014)677.
[5]. S. Borisenko, Q. Gibson, D. Evtushinsky, V. Zabolotnyy, B. Büchner, R. J. Cava. Phys. Rev. Lett. 113(2014)027603.
[6]. A. V. Kochura, L. N. Oveshnikov, A. P. Kuzmenko, A. B. Davydov, S. Yu. Gavrilkin, V. S. Zakhvalinskii, V. A. Kulbachinskii, N. A. Khokhlov, B. A. Aronzon. JETP Letters. 109(2019)175.
[7]. A.V. Galeeva, I.V. Krylov, K.A. Drozdov, A.F. Knjazev, A.V. Kochura, A.P. Kuzmenko, V.S. Zakhvalinskii, S.N. Danilov, L.I. Ryabova, D.R. Khokhlov. Beilstein Journal of Nanotechnology. 8(2017)167.
[8]. H. Lu, X. Zhang, Y. Bian, Sh. Jia. Scientific Reports 7(2017)3148.
[9]. E.K. Arushanov. Prog. Crystal Growth Charact. 3(1981)211.
[10]. N. F. Mott, Metal–Insulator Transitions, London: Taylor and Francis (1990).
[11]. Mott N.F., Davies E.A. Electron Processes in Non-Crystalline Materials. - Oxford: Clarendon, 1979;
[12]. Shklovskii B.I., Efros A.L. Electronic Propertie of Doped Semiconductors. - Berlin: Springer-Verlag, 1984.

Эксперимент

Получение керамических образцов $La_{0.5}Sr_{0.5}Mn_{1-y}Fe_yO_3$ и исследование механизмов электропроводности

Керамические образцы $La_{0.5}Sr_{0.5}Mn_{0.9}Fe_{0.1}O_3$ и $La_{0.5}Sr_{0.5}MnO_3$ были получены с применением стандартной твердофазной реакции. Для синтеза использовались исходные материалы La_2O_3, MnO_2, Fe_2O_3 и $SrCO_3$. Смеси порошков исходных материалов отжигались на воздухе пр
межуточным измельчением. Полученный порошок прессовался в таблетки под давлением 2000 кг/см2, затем таблетки отжигались на воздухе при температуре 1360°C в течение 22 часов. В соответствии с результатами рентгенофазового анализа было установлено, все образцы со
$La_{0.5}Sr_{0.5}MnO_3$ R-3c, hexagonal , a = 5.473408 , b = 5.473408 , c = 13.345732; $La_{0.5}Sr_{0.5}Mn_{0.9}Fe_{0.1}O_3$ R-3c, hexagonal, a = 5.477067, b = 5.477067, c = 13.353921;

Измерения электропроводности и магнетосопротивления были проведены на автоматизированной установке замкнутого цикла (Mini Cryogen Free Measurements System (Cryogenic Ltd, UK)) в интервале температур 20 ÷ 300 K и в магнитном поле до 1 Тл. Полученные темпера
нетосопротивления керамических образцов $La_{0.5}Sr_{0.5}MnO_3$ и $La_{0.5}Sr_{0.5}Mn_{0.9}Fe_{0.1}O_3$ (см. Fig. 1 (Abstract) и Рис. 3) существенно отличались от исследованных ранее образцов $La_{0.7}Sr_{0.3}Mn_{1-y}Fe_yO_3$ с содержанием железа $0.03 \le y \le 0.25$ [3]. В обоих исследованных образцах наблюдало
время как в системе твёрдых растворов $La_{0.7}Sr_{0.3}Mn_{1-y}Fe_yO_3$ наблюдался эффект колоссального магнетосопротивления (подавления сопротивления образца внешним полем). Легирование железом приводило к росту удельного сопротивления, сопровождающееся превращением м
вационную при y= 0.25.

Для керамических образцов $La_{0.5}Sr_{0.5}MnO_3$ были установлены температурные диапазоны и тип прыжковой проводимости, указано сопротивление ρ_0 и энергия активации Ea, (см. Тблицу1)
Как видно из сравнения рис. 4,рис. 5, рис. 6 и Fig 1 и (Abstract) легирование 10% Fe приводит к сильному изменению температурной зависимости соротивления в нулевом и магнитном поле 1Тл. Легирование железом привело к исчезновению низкотемпературного участка пры
водимости с переменной длинной прыжка по Шкловскому –Эфрос сместился в более высокме температуры.

Discussion

The analysis of the experimental neutron diffraction patterns $La_{0.7}Ca_{0.3}Mn_{0.5}Fe_{0.5}O_3$ sample (see Fig.3) indicates on the formation of antiferromagnetic long-range ordering G-type [10]. In the AFM phase of G-type direction of the magnetic moment of each Mn ion opposite to the direction of th parently from Fig. 3, in the samples with decreasing temperature there is an increase in the peak intensity at the interplanar spacing d = 4.45 Å which indicates the formation of antiferromagnetic ordering of the G-type. Analysis of the temperature dependence of the average magnetic moments of io tion temperature in the AFM state of the G-type is 350 K for $La_{0.7}Ca_{0.3}Mn_{0.5}Fe_{0.5}O_3$. The magnetic moments of one Mn / Fe ion accounted 0.9 μB at 10 K. Throughout the temperature range 10 ÷ 300 K has not been detected appearance additional contribution to the intensity of the nuclear peaks a ferromagnetism in manganite perovskites [11].Thus, from a comparison of the results of the analysis of experimental neutron diffraction patterns and temperature dependence of the magnetization, $M(T)$ $La_{0.7}Ca_{0.3}Mn_{0.5}Fe_{0.5}O_3$ sample we conclude that the antiferromagnetic long-range ordering G- perature in 350 K . With decreasing temperature there is an increase in the neutron diffraction patterns peak intensity the AFM state of the G-type and simultaneously the temperature dependence of the magnetization, $M(T)$ suggests the frustration of magnetic ground state and the existence of a spi